energies

*Perspective*

# New Trends in the Control of Grid-Connected Photovoltaic Systems for the Provision of Ancillary Services

**Jose Miguel Riquelme-Dominguez [1], Jesús Riquelme [2,*] and Sergio Martinez [1]**

[1] Department of Electrical Engineering, Escuela Técnica Superior de Ingenieros Industriales, Universidad Politécnica de Madrid, 28040 Madrid, Spain
[2] Department of Electrical Engineering, Universidad de Sevilla, 41004 Seville, Spain
* Correspondence: jsantos@us.es

**Abstract:** The gradual displacement of conventional generation from the energy mix to give way to renewable energy sources represents a paradigm shift in the operation of future power systems: on the one hand, renewable technologies are, in general, volatile and difficult to predict; and on the other hand, they are usually connected to the grid through electronic power converters. This decoupling due to power converters means that renewable generators lack the natural response that conventional generation has to the imbalances between demand and generation that occur during the regular operation of power systems. Renewable generators must, therefore, provide a series of complementary services for the correct operation of power systems in addition to producing the necessary amount of energy. This paper presents an overview of existing methods in the literature that allow photovoltaic generators to participate in the provision of ancillary services, focusing on solutions based on power curtailment by modifying the traditional maximum power point tracking algorithm.

**Keywords:** active power reserves; ancillary services; maximum power point tracking (MPPT); power curtailment; solar photovoltaics (PV)



**Citation:** Riquelme-Dominguez, J.M.;Riquelme, J.; Martinez, S. New Trends in the Control of Grid-Connected Photovoltaic Systems for the Provision of Ancillary Services. *Energies* **2022**, *15*, 7934. https://doi.org/10.3390/en15217934

Academic Editor: Carlo Renno

Received: 23 September 2022
Accepted: 23 October 2022
Published: 26 October 2022



## 1. Introduction

Since the invention of electricity as a source of energy in the late 19th century, the generation of this kind of energy has been mainly carried out through fossil fuels such as oil, gas, and coal [1]. However, this energy mix has been questioned in the last decades. It has been proved that the combustion of hydrocarbons for electricity production is primarily responsible for the emission of greenhouse gases into the atmosphere, causing the imminent problem of global warming [2,3].

Removing carbon dioxide emissions and reducing fossil fuel reserves has led to the gradual displacement of conventional energy sources to make way for renewable energy technologies. Figure 1 depicts the evolution of the installed capacity in the European Union by generation technology, with projections up to 2040 [4].

The paradigm shift is evident: non-conventional energy sources will dominate future power systems. However, besides the environmental benefits provided by renewable energies, managing this kind of energy is more complex than managing traditional energy sources. On the one hand, the intermittent character of renewable resources makes their forecasting volatile and, to a certain extent, unpredictable [5]. On the other hand, in contrast to conventional generators, which are directly connected to the grid, renewable generators are decoupled from power systems by employing electronic converters, thus reducing the synchronous equivalent inertia of the system [6]. The latter characteristic is essential to determine the behavior of power systems in case of disturbances due to generator tripping or connection and disconnection of a large amount of load.

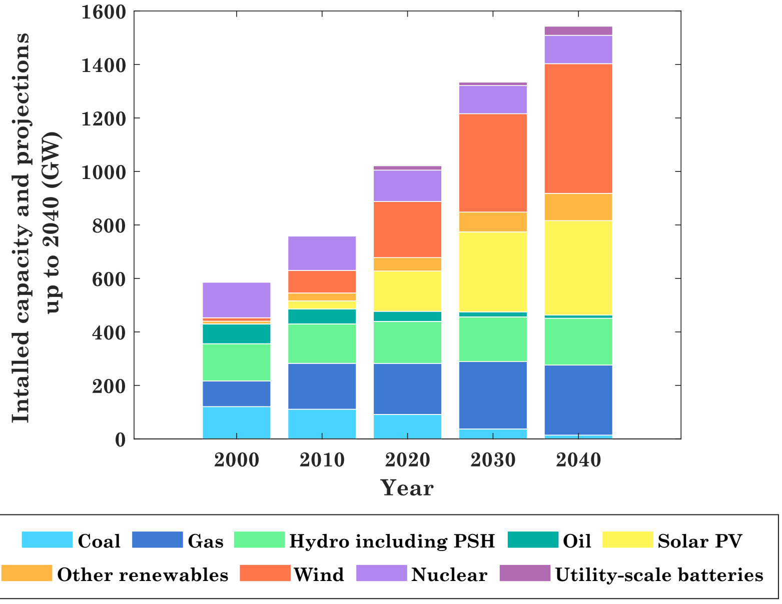


**Figure 1.** Installed capacity (GW) in the European Union by generation technologies (2000–2010) and projections up to 2040 in the Sustainable Development Scenario.

In alternating-current power systems, the rotating speed of the operational synchronous generation, $\omega_r$, determines the frequency of the characteristic voltage waveform (50 or 60 Hz). Under steady-state conditions, all synchronous generators in the system rotate at such an angular velocity that, when multiplied by their respective number of pole pairs, $p$, they produce a single value of angular pulsation, $\omega_s = \omega_r\, p$. Therefore, from the point of view of frequency ($f_s = \omega_s / (2\,\pi)$), all generators are spinning at a single speed, i.e., they operate in synchronism.

At the same time, frequency deviation from its nominal value in a power system is closely related to the difference between power generated and power demand. This relationship can be seen in a very illustrative way by considering a synchronous generator driven by a turbine and feeding an isolated electric load, as shown in Figure 2. Suppose mechanical and electrical losses are ignored in steady-state. In that case, the mechanical power transmitted to the generator shaft by the turbine, $P_m$, is equal to the electrical power demanded at the generator terminals, $P_e$. If, suddenly, the electrical power consumed by the load increases its value, keeping unchanged the value of the mechanical power exerted by the primary drive, this increase in demanded power is assumed by the generator by making use of the kinetic energy stored in its rotor. This expenditure of kinetic energy decreases the rotational speed of the machine, with the consequent drop in frequency.

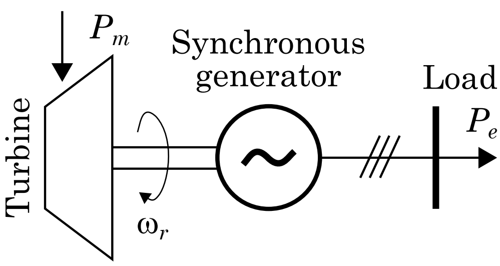


**Figure 2.** Electric generator feeding an isolated load.

The angular velocity of a synchronous generator depends on the difference between generated and demanded power and can be expressed analytically by employing the oscillation equation of a synchronous generator [7]:

$$\Delta P_m - \Delta P_e = 2\,H \frac{\partial}{\partial t} \Delta\omega_r \quad (1)$$

Equation (1) defines a synchronous generator's rotational dynamics, considering small variables' small deviations from their steady-state value. Power imbalance in a synchronous generator is translated into a variation of its angular velocity, whose rate of change is conditioned by the inertia constant of its rotating masses, $H$.

As previously stated, conventional synchronous generators respond to mismatches in the demand–generation balance. However, renewable generators lack this capability due to electronic converter decoupling. To understand this difference, let us consider the same isolated load as in the previous example, but now powered by a two-stage photovoltaic (PV) system, as shown in Figure 3.

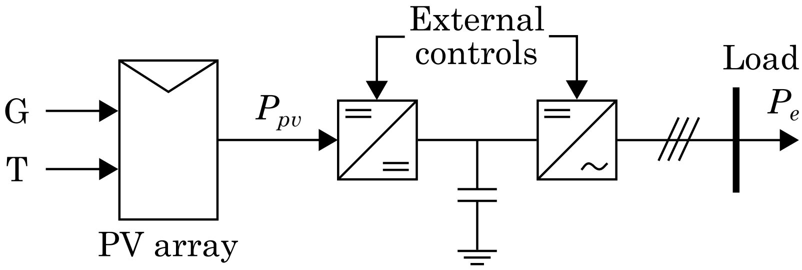


**Figure 3.** PV system feeding an isolated load.

The availability of the renewable resource, characterized by the atmospheric conditions of irradiance, $G$, and temperature, $T$, determines the generating capacity of a PV array. To optimize the renewable resource, the DC–DC converter is usually equipped with a maximum power point tracking (MPPT) algorithm, ensuring the system generates the maximum power available at any given time. Let us now assume that the losses in the converters are negligible and that the power demanded by the load, $P_e$, coincides with the power delivered by the panel, $P_{pv}$. If the load suddenly increases the power demand, the PV system cannot increase its output, which breaks the demand–generation balance, causing a continuous drop in frequency. Alternatively, while the system is operating at steady state, a reduction in renewable resources may occur, for example, due to the passage of a cloud, affecting the generation–demand balance. Finally, renewable generators do not contribute to increasing the inertia of the power system since they are decoupled from it, resulting in faster and more severe frequency excursions.

Therefore, high penetration of non-conventional energy in power systems implies lower capacity to respond to demand–generation mismatches in the normal operation of power systems, affecting the condition and the security of the power supply [8,9]. Hence, the objective is to expand the use of renewable energy in power systems while maintaining efficiency and robustness. To achieve this purpose, other than providing the necessary amount of energy to meet the demand, renewable generators must participate in supplying ancillary services, regarded as those operations critical to ensuring the safe functioning and reliability of power networks.

Numerous research articles on ancillary services provided by renewable generators may be found in the literature, with solar and wind generators standing out [10,11]. In particular, photovoltaic technology has several features that make it a prime choice for offering auxiliary services to power networks. Compared to other renewable generators, these features include less maintenance time, fully integrated power electronics that allow quick response, and lack of spinning masses that increase the response time [12]. In recent years, several contributions regarding photovoltaic systems support the inertial response, and primary frequency control has been proposed in the literature [13,14], a sign of the subject's current relevance. Two methodologies allow ancillary services to integrate photovoltaic energy: using energy storage systems [15,16] or operating photovoltaic systems below their maximum power point (MPP). Both approaches are different alternatives to be evaluated on each installation, taking into consideration various aspects such as energy price, additional equipment costs, capital costs, or even economic compensation or obligation for providing ancillary services. Even though the power curtailment technique implies energy waste, it takes less initial investment, making it a different option to take into account given the singularity of each installation. Additionally, deliberated power reduction and storage are not always mutually exclusive approaches, since in some circumstances, combining the two results in the most helpful answer from an economic standpoint [17].

Figure 4 shows the P–V curve of a PV system under uniform irradiance and temperature conditions. On the curve, it is possible to identify the MPP, the coordinates of which are ($V_{MPP}$, $P_{MPP}$). To maintain active power reserves without installing energy storage systems, it is necessary to discharge the operating point at a level below the MPP, for example, $P_{curtailed}$. As can be seen, there are two possible alternatives for operating at $P_{curtailed}$: to the left and to the right of the MPP. While working at a deloaded point, the PV system can provide support for over-frequency (moving further away from the MPP) and under-frequency (moving closer to the MPP) events, as shown in Figure 4.

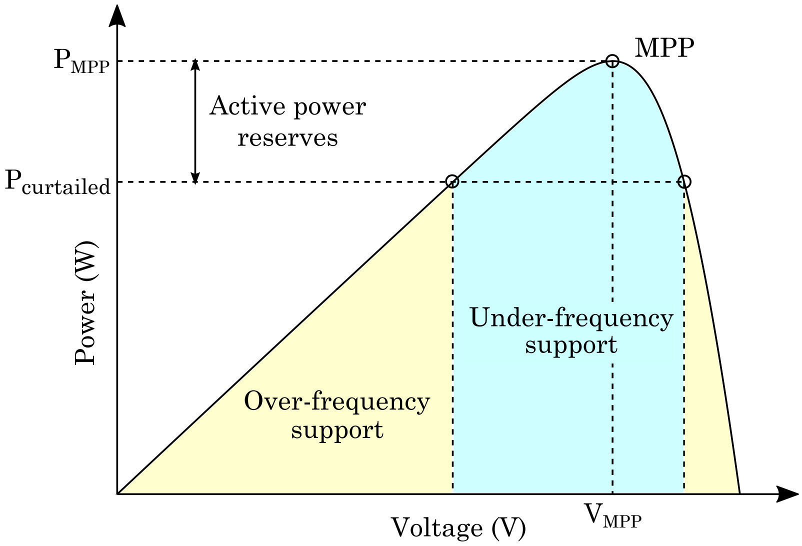


**Figure 4.** Power–voltage curve of a photovoltaic system under uniform environmental conditions. MPP versus curtailed operating points.

This paper presents the most recent developments in power-curtailed operation of PV systems, focusing on the following:

1. How different methods determine the maximum available power while operating below that point'
2. Implementation details, such as additional equipment required or the most appropriate plant size for one type of control'
3. The application the control is designed for. For example constant power generation, power reserves control, power ramp-rate control, or virtual inertia control.

The remainder of this paper is organized as follows: Section 2 introduces the traditional control of grid-connected photovoltaic systems. Section 3 details the most recent alternatives for flexible control of grid-connected photovoltaic systems. A brief description of each method and a comparison between them is included. The main recommendations of the authors are summarized in Section 4. Finally, Section 5 concludes the work.

## 2. Traditional Control of Grid-Connected Photovoltaic Systems

Photovoltaic systems are usually connected to the grid through a system similar to the one shown in Figure 5. This system consists of two conversion stages. The first one, consisting of a DC–DC converter, is responsible for raising the output voltage of the PV array to the levels required by the inverter. Additionally, this first converter is where the MPPT algorithm is implemented. MPPT algorithms try to optimize PV production, which is highly dependent on the atmospheric conditions of irradiance and temperature, by varying the duty cycle of the DC–DC converter depending on the current and voltage measurements obtained from the PV generator. There is a wide variety of MPPT algorithms of different natures depending on how they perform MPP measurement, estimation, and tracking [18].

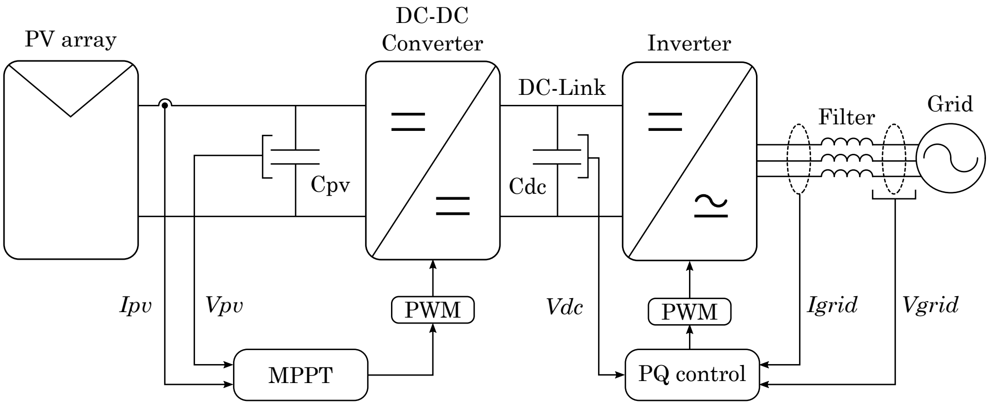


**Figure 5.** Traditional control of grid-connected photovoltaic systems.

In the second conversion stage, which is carried out by the inverter, the voltage and current magnitudes are transformed into alternating current magnitudes so they can be injected into the grid. For this purpose, the inverter control takes measurements of the DC link voltage and the currents and voltages at the output of the filter. In the inverter, it is usual to implement a PQ control to provide the power demanded by the grid.

However, as mentioned above, the production of the PV system is strongly dependent on the atmospheric conditions and, more specifically, on the irradiance incident on the panel, as it usually has high-speed dynamics due to the passage of clouds over the solar array. This problem, reported not only in small PV installations but also in large-scale plants [19], negatively impacts the grid's performance. Therefore, sudden changes in the incident irradiance imply changes in the generated power. If the grid demands constant active power, sudden changes in the generated PV power change the DC-link voltage, which usually has a minimal operating range due to the requirements of the converters to which it is connected.

## 3. Alternative Control of Grid-Connected Photovoltaic Systems

As explained in the previous section, it seems reasonable to modify the traditional MPPT algorithms so that PV systems can have the margin to inject more or less power into the grid, thus reducing power oscillations due to irradiance fluctuations. Recently, different control techniques have been proposed to achieve this goal, which can be grouped into the categories described in Figure 6.

The following subsections describe the main methods available in the literature for photovoltaic power curtailment.

### *3.1. Methods Based on a System Operator Command*

Some techniques rely on the system operator (SO) to control PV plants below the MPP. The work presented in [20] implements a flexible power point tracking (FPPT) algorithm to get the PV system to participate in the power ramp-rate control (PRRC) service. The control system receives the suboptimal operating voltage from the SO, which implies that this method is designed for medium–large size PV plants. In addition, grid codes impose the maximum allowed power ramp-rate. With this information, the PV plant is regulated through a modified P&O algorithm to fulfill the grid requirements.

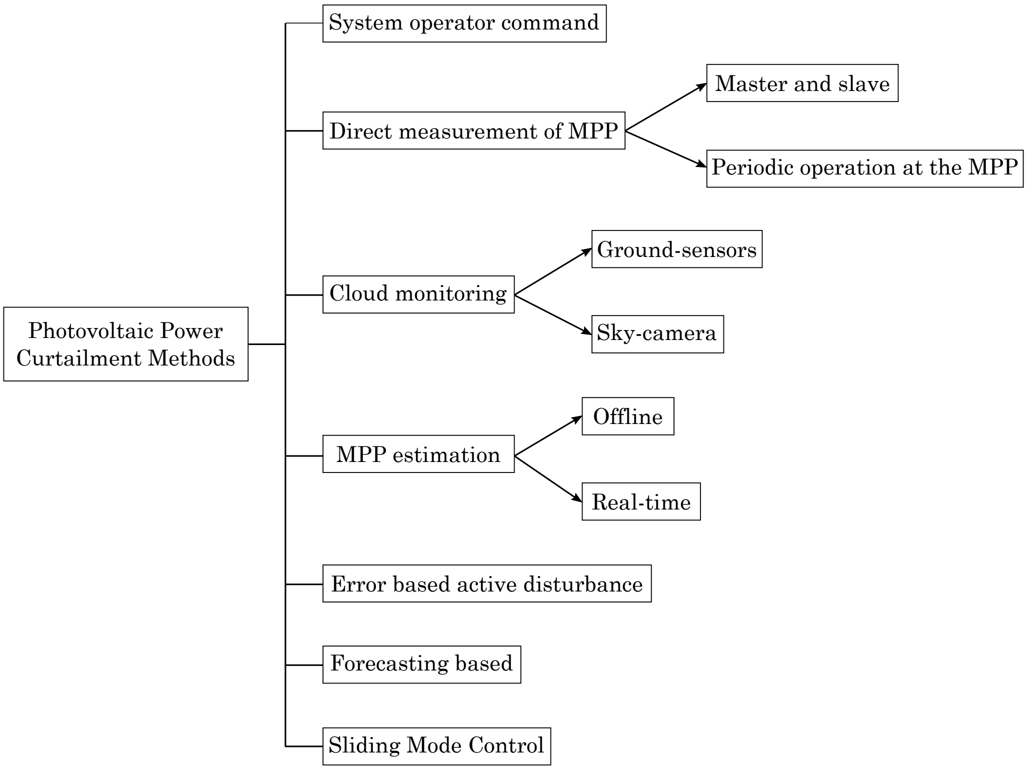


**Figure 6.** Classification of PV power curtailment methods depending on the determination of the MPP.

A different approach within this category consists of the use of distributed power reserves [21], in which a PV plant is divided into subsystems (clusters), and the power reserves are distributed over the clusters on a decentralized basis. This procedure is particularly interesting as the drop in power generation in one group can be compensated by pushing the operating point of another cluster nearer to its MPP, achieving a constant power generation (CPG) control mode. A complete DC microgrid stability analysis is accomplished to evaluate the adjustment of the power curtailed set-points.

### *3.2. Methods Based on Direct Measurement of the MPP*

The authors of [22] implement the so-called "master and slave" technique in a multi-string PV configuration so that one string is dedicated to operating at its MPP. In contrast, the remaining strings are operated below the maximum available power. One merit of this method is that if the PV strings are identical and the system works under uniform environmental conditions, the MPP is accurately determined. Although as PV plant size increases, the MPP measurement may be less accurate due to partial shading conditions, in the case of large plants, several master strings can be arranged throughout the system.

An alternative strategy consists of moving the operating point to the MPP recursively [23]. Once the MPP is directly measured through the general perturb and observe (P&O) algorithm, one variant of the P&O algorithm dedicated to direct control of PV power is used to set the operating point on the left part of the P–V curve, providing the required level of reserves. In this manner, the photovoltaic system can work in a power reserve control (PRC) mode. This method has the advantage of measuring the MPP very accurately, but it involves more curtailment than the method in [22]. However, it does not require any additional equipment.

The method in [24] expanded the above-mentioned technique to consider PV systems under partial shading conditions. Partial shading conditions mean that PV systems do not have a single MPP but have several local maxima along the P–V curve. In this method, when a change in environmental conditions is detected, global maximum power point tracking (GMPPT) is applied, and the maximum available power is directly measured.

Then, depending on the desired operation mode, CPG or PRC, the power reference is set and achieved through PV voltage control.

### 3.3. Methods Based on Cloud Monitoring

The work presented in [25] incorporates a ground-based sensor forecasting system (GBSFS) and develops a dynamic spatio–temporal ramp-forecasting algorithm to limit photovoltaic power ramps. GBSFS is formed by six sensors consisting of six short-circuited solar cells, which predict the movement of the clouds above the PV system and, therefore, act accordingly to regulate the operating point to the right of the P–V curve. Due to additional equipment, this method is more suitable for medium to large PV plants. A similar alternative to the above is presented in [26], but instead of GBSFS, it uses sky cameras to predict cloud movement.

### 3.4. Methods Based on Maximum Power Point Estimation

Offline MPP estimation is carried out in [27]. The data are preloaded in a 3D look-up table. Then, in real-time, trilinear interpolation is used together with irradiance and temperature measurements to determine the suboptimal operating point. This point usually lies on the right part of the P–V curve. Consequently, the system cost is increased due to the additional sensors, which makes this alternative useful for large PV plants.

The authors of [28] improved the method mentioned above by using real-time least-squares curve-fitting estimation of the MPP and the complete P–V curve. Ripple control is added to provide an adequate measurement window for appropriate estimation. Although this method implies a high calculation burden, it has been proven in a commercial micro-controller, which means that the presented technique is ready to be implemented in real PV plants, irrespective of their size.

A straightforward method is proposed in [29] to estimate the MPP in real time. Only two voltage–current measurements are needed in the constant current region (to the left of the MPP), where the $I$–$V$ curve is nearly linear. It is then simple to calculate the short-circuit current, and finally, an empirical expression is used to get the MPP. Although this method is quick and straightforward, it is unstable when there is measurement noise.

The possibility of operating the PV system suboptimally on both the left and right sides of the P–V curve was introduced in [30]. This work also demonstrated that real-time estimation of irradiance and temperature highly depends on the operation side. Near the MPP, both irradiance and temperature can be estimated accurately. However, if the operating point is far from the MPP on the left side of the P–V curve, temperature estimation is trapped in a local minimum. The same occurs for the irradiance estimation if the operating point falls on the right part of the curve. The previous work was complemented in [31] by considering the power losses in the grid-connection converter stages. With that contribution, MPP estimation is determined from the grid's point of view.

An alternative approach was introduced recently in [32]. This method needs just one PV current measurement to have a rough estimate of the system's short-circuit current. Using the linear relation between that current and the MPP, it gets a first approximation of the MPP. In successive steps, the method refines that estimation. The suboptimal operating point lies on the left part of the P–V curve, and the tracking algorithm uses a variable-size voltage control to have a high tracking speed. This control technique has been applied to virtual inertia control (VIC) and droop control emulation.

The method presented in [33] uses MPP estimation while operating suboptimally to control photovoltaic power ramps. It works on the right side of the P–V curve through direct power control and regulates PV power following the maximum power ramp-rate permitted. With this method, positive power ramps are always limited. However, the proper control of power ramp-down is directly related to the previous level of curtailment.

### *3.5. Methods Based on Error-Based Active Disturbance*

Constant power generation control based on the P&O algorithm is improved in [34] using error-based active disturbance (EBAD) control in terms of dynamic performance and power oscillations. The control system is tested in different environmental conditions and in various operation modes and considers operation on both sides of the P–V curve. The control parameters are tuned through the double-quantum chaotic social spider optimization algorithm.

### *3.6. Methods Based on Forecasting*

The method presented in [35] allows VIC based on irradiance forecasting so that several PV plants participate in a coordinated reserve strategy. Based on forecasting results, if a large irradiance excursion is predicted for one PV plant, the remaining ones curtail their generation to provide VIC.

### *3.7. Methods Based on Sliding Mode Control*

A novel method based on sliding mode control (SMC) is proposed in [36]. For the proper functioning of SMC, a sliding mode surface needs to be defined as a function of the quotient $\partial P_{pv}/\partial V_{pv}$. The parameters of this controller are tuned to emulate the drop characteristic of a synchronous generator, as its main application is to get the PV plants to participate in primary frequency regulation (PFR). Apart from the fact that it does not require any additional equipment, an advantage of this method is that it can operate in MPPT mode or in adaptive power point tracking (APPT) in a continuous way, avoiding switching between operation modes.

## 4. Recommendations of the Authors

As reviewed, trends in the control of grid-connected PV systems are evolving to provide ancillary services to the grid. In this paper, classification based on the way each method determines the available power while operating in the curtailed mode is introduced. Table 1 summarizes the main characteristics of the PV power curtailment approaches, including the operation side on the P–V curve of each technique, the suitability of each technique depending on the size of the photovoltaic system, the additional equipment required for the correct functioning of the methods, and the application for which they are designed.

**Table 1.** Summary of the main methods for photovoltaic power curtailment.

| Method | Classification | Operation Side | PV System Size | Additional Equipment | Application |
|---|---|---|---|---|---|
| [20] | System operator command | Left | Large | No | PRRC |
| [21] | System operator command | Right | Large | No | CPG |
| [22] | Direct measurement of MPP | Right | Small, large | Communication systems | CPG |
| [23] | Direct measurement of MPP | Left | Small, large | No | PRC |
| [24] | Direct measurement of GMPP | Left, right | Small, large | No | CPG, PRC |
| [25] | Cloud monitoring | Right | Large | GBSFS | PRRC |
| [26] | Cloud monitoring | Right | Large | Sky camera | PRRC |
| [27] | MPP estimation | Right | Small, large | Irradiance and temperature sensors | PRC |
| [28] | MPP estimation | Right | Small, large | No | PRC |
| [29] | MPP estimation | left | Small, large | No | PRC |
| [30] | MPP estimation | Left, right | Small, large | No | PRC |
| [32] | MPP estimation | Left | Small, large | No | VIC, Droop control |
| [31] | MPP estimation | Left | Small, large | No | PRC |
| [33] | MPP estimation | Right | Small, large | No | PRRC |
| [34] | Error-based active disturbance | Left, right | Small, large | No | CPG |
| [35] | Forecasting-based | Right | Large | No | VIC |
| [36] | Sliding mode control | Left | Small, Large | No | PFR |

Methods based on a system operator command are specifically designed for large PV plants with high installed capacity. The power command must be converted in a voltage reference to be used in the FPPT of each inverter of the plant, as usually the operator ignores the P–V curve of the PV system. However, it is essential to note that if the SO has no access to short-term irradiance forecasting, it may require more power than available. Therefore, this technique is preferable to be used with real-time irradiance measurements and forecasting.

Direct measurement of the MPP is suitable for small to large PV systems, as just one PV panel is enough to determine the available power. The main disadvantage of this method is that the PV system needs identical PV modules, which is not always possible. In addition, the accuracy of this method is subject to thorough maintenance and how the elements of the system age. The MPP measurement can be highly accurate if these facts are carefully monitored.

Cloud monitoring is feasible when the size of the PV system is significant. This technique predicts the movement of the clouds and, therefore, the evolution of the maximum power available. It is worth noting that ground-based sensors are more accurate than sky cameras for short-term operation (from minutes to one hour). On the other hand, sky cameras are more suitable if the prediction horizon is more than one hour. The main disadvantage of these techniques is the use of additional equipment.

Estimating the MPP in real-time is the most common solution for curtailed operation of PV systems. Various methods assess the MPP through different mathematical models, from the simplest to the most complex. Simple methods are generally less accurate than complex ones, but they offer a fair solution when the priority is to have a cost-effective system. Complex models are used when accuracy is crucial, so the estimation is carried out with a large measurement window that minimizes the error due to measurement noise.

Short-term irradiance forecasting can be used to predict the evolution of the available power in a PV plant. To have an accurate model, it is necessary to have large amounts of data, such as high-resolution irradiance data, wind speed data, and historical energy production data. If this information is available and the models have been trained adequately, irradiance forecasting is a tool to be considered. One disadvantage of this method is the aging of PV modules and the maintenance of the plant.

Sliding mode control has the advantage that the sliding mode surface can be computed offline and real-time operation can be done without additional equipment. Apart from the aging problem, which can force the model to update once per year, this method requires sensible measurements of the power derivative with respect to voltage, which can be highly affected by the measurement noise.

Although the variety of the reviewed methods is quite wide, each has advantages and drawbacks in terms of accuracy, installation and maintenance cost, and suitability for one specific PV plant size. From our point of view, simple but accurate techniques such as master and slave are balanced solutions that may be further explored. In addition, with the deployment of PV systems around the world, from domestic generators to PV farms, large amounts of data can be collected to apply artificial intelligent methods to have high accurate forecasting models that grid-connected PV system controllers can use.

## 5. Conclusions

The wide deployment of installed solar PV capacity has changed the way these systems are operated: from traditional MPPT algorithms to more flexible control algorithms that allow the PV systems to provide additional services to the grid. In this sense, several contributions have, in very recent years, proposed new techniques to achieve this goal. This paper presents classification of these contemporary methods, with a brief description and a comparison between them. The selection of one of these methods for a particular application will depend on factors such as the size of the PV system, the possibility of acquiring additional equipment, or the control objective. We recommend simple but accurate techniques such as master and slave and irradiance forecasting models to predict the maximum available power on short-term horizons. Future studies should investigate specific cases in which different techniques are compared under the same conditions to analyze the performance of each one. This analysis will help determine the most appropriate solution for each application.

**Author Contributions:** Conceptualization, J.M.R.-D., J.R. and S.M.; Data curation, J.M.R.-D.; Formal analysis, J.M.R.-D., J.R. and S.M.; Funding acquisition, J.R. and S.M.; Investigation, J.M.R.-D.; Methodology, J.M.R.-D., J.R. and S.M.; Project administration, J.R. and S.M.; Software, J.M.R.-D.; Supervision, S.M.; Validation, J.M.R.-D.; Visualization, J.M.R.-D.; Writing—original draft, J.M.R.-D.; Writing—review & editing, J.M.R.-D., J.R. and S.M. All authors have read and agreed to the published version of the manuscript.

**Funding:** This research has been funded by the Spanish Ministry of Economy and Competitiveness under the projects AEI PID2019-108966RB-I00 and TED2021-131311B-C21. Also by the Andalusian Regional Government under the project PYC20 RE 078 US.

**Data Availability Statement:** Not applicable.

**Conflicts of Interest:** The authors declare no conflict of interest.

## Abbreviations

The following abbreviations are used in this manuscript:

| | |
|---|---|
| APPT | adaptive power point tracking |
| CPG | constant power generation |
| FPPT | flexible power point tracking |
| GBSFS | ground-based sensor forecasting system |
| GMPPT | global maximum power point tracking |
| MPP | maximum power point |
| MPPT | maximum power point tracking |
| P&O | perturb and observe |
| PFR | primary frequency regulation |
| PRC | power reserve control |
| PRRC | power ramp-rate control |
| PV | photovoltaic |
| SMC | sliding mode control |
| SO | system operator |
| VIC | virtual inertia control |

## References

1. Zou, C.; Zhao, Q.; Zhang, G.; Xiong, B. Energy revolution: From a fossil energy era to a new energy era. *Nat. Gas Ind. B* **2016**, *3*, 1–11. [CrossRef]
2. Hardisty, P.E.; Clark, T.S.; Hynes, R.G. Life Cycle Greenhouse Gas Emissions from Electricity Generation: A Comparative Analysis of Australian Energy Sources. *Energies* **2012**, *5*, 872–897. [CrossRef]
3. Tajeddin, A.; Roohi, E. Designing a reliable wind farm through hybridization with biomass energy. *Appl. Therm. Eng.* **2019**, *154*, 171–179. [CrossRef]
4. IEA. *Installed Capacity in the European Union, 2000–2010. and Projections up to 2040 in the Sustainable Development Scenario*; Technical Report; International Energy Agency: Paris, France, 2020.
5. Mohandes, B.; Moursi, M.S.E.; Hatziargyriou, N.; Khatib, S.E. A Review of Power System Flexibility with High Penetration of Renewables. *IEEE Trans. Power Syst.* **2019**, *34*, 3140–3155. [CrossRef]
6. Fang, J.; Li, H.; Tang, Y.; Blaabjerg, F. On the Inertia of Future More-Electronics Power Systems. *IEEE J. Emerg. Sel. Top. Power Electron.* **2019**, *7*, 2130–2146. [CrossRef]
7. Kundur, P.; Balu, N. *Power System Stability and Control*, 1st ed.; McGraw-Hill: New York, NY, USA, 1994.
8. Sigrist, L.; Egido, I.; Lobato Miguélez, E.; Rouco, L. Sizing and Controller Setting of Ultracapacitors for Frequency Stability Enhancement of Small Isolated Power Systems. *IEEE Trans. Power Syst.* **2015**, *30*, 2130–2138. [CrossRef]
9. Nguyen, N.; Mitra, J. Effect of wind power on load frequency control. In Proceedings of the 2016 IEEE Power and Energy Society General Meeting (PESGM), Boston, MA, USA, 17–21 July 2016; pp. 1–5. [CrossRef]
10. Batzelis, E.I.; Anagnostou, G.; Cole, I.R.; Betts, T.R.; Pal, B.C. A State-Space Dynamic Model for Photovoltaic Systems with Full Ancillary Services Support. *IEEE Trans. Sustain. Energy* **2019**, *10*, 1399–1409. [CrossRef]
11. Van de Vyver, J.; De Kooning, J.D.M.; Meersman, B.; Vandevelde, L.; Vandoorn, T.L. Droop Control as an Alternative Inertial Response Strategy for the Synthetic Inertia on Wind Turbines. *IEEE Trans. Power Syst.* **2016**, *31*, 1129–1138. [CrossRef]
12. Crăciun, B.I.; Kerekes, T.; Séra, D.; Teodorescu, R. Frequency Support Functions in Large PV Power Plants with Active Power Reserves. *IEEE J. Emerg. Sel. Top. Power Electron.* **2014**, *2*, 849–858. [CrossRef]
13. Li, Q.; Baran, M.E. A Novel Frequency Support Control Method for PV Plants Using Tracking LQR. *IEEE Trans. Sustain. Energy* **2020**, *11*, 2263–2273. [CrossRef]

14. Zhong, C.; Zhou, Y.; Yan, G. A Novel Frequency Regulation Strategy for a PV System Based on the Curtailment Power-Current Curve Tracking Algorithm. *IEEE Access* **2020**, *8*, 77701–77715. [CrossRef]
15. Sukumar, S.; Marsadek, M.; Agileswari, K.R.; Mokhlis, H. Ramp-rate control smoothing methods to control output power fluctuations from solar photovoltaic (PV) sources—A review. *J. Energy Storage* **2018**, *20*, 218–229. [CrossRef]
16. Martins, J.; Spataru, S.; Sera, D.; Stroe, D.I.; Lashab, A. Comparative study of ramp-rate control algorithms for PV with energy storage systems. *Energies* **2019**, *12*, 1342. [CrossRef]
17. Solomon, A.; Bogdanov, D.; Breyer, C. Curtailment-storage-penetration nexus in the energy transition. *Appl. Energy* **2019**, *235*, 1351–1368. [CrossRef]
18. Li, X.; Wang, Q.; Wen, H.; Xiao, W. Comprehensive Studies on Operational Principles for Maximum Power Point Tracking in Photovoltaic Systems. *IEEE Access* **2019**, *7*, 121407–121420. [CrossRef]
19. Cormode, D.; Cronin, A.D.; Richardson, W.; Lorenzo, A.T.; Brooks, A.E.; DellaGiustina, D.N. Comparing ramp rates from large and small PV systems, and selection of batteries for ramp rate control. In Proceedings of the 2013 IEEE 39th Photovoltaic Specialists Conference (PVSC), Tampa, FL, USA, 16–21 June 2013; pp. 1805–1810. [CrossRef]
20. Li, X.; Wen, H.; Chen, B.; Ding, S.; Xiao, W. A cost-effective power ramp rate control strategy based on flexible power point tracking for photovoltaic system. *Sol. Energy* **2020**, *208*, 1058–1067. [CrossRef]
21. Khan, A.; D'silva, S.; Fard, A.Y.; Shadmand, M.B.; Abu-Rub, H. On Stability of PV Clusters with Distributed Power Reserve Capability. *IEEE Trans. Ind. Electron.* **2021**, *68*, 3928–3938. [CrossRef]
22. Sangwongwanich, A.; Yang, Y.; Blaabjerg, F.; Sera, D. Delta Power Control Strategy for Multistring Grid-Connected PV Inverters. *IEEE Trans. Ind. Appl.* **2017**, *53*, 3862–3870. [CrossRef]
23. Peng, Q.; Tang, Z.; Yang, Y.; Liu, T.; Blaabjerg, F. Event-Triggering Virtual Inertia Control of PV Systems with Power Reserve. *IEEE Trans. Ind. Appl.* **2021**, *57*, 4059–4070. [CrossRef]
24. Tafti, H.D.; Wang, Q.; Townsend, C.D.; Pou, J.; Konstantinou, G. Global Flexible Power Point Tracking in Photovoltaic Systems Under Partial Shading Conditions. *IEEE Trans. Power Electron.* **2022**, *37*, 11332–11341. [CrossRef]
25. Chen, X.; Du, Y.; Wen, H.; Jiang, L.; Xiao, W. Forecasting-Based Power Ramp-Rate Control Strategies for Utility-Scale PV Systems. *IEEE Trans. Ind. Electron.* **2019**, *66*, 1862–1871. [CrossRef]
26. Saleh, M.; Meek, L.; Masoum, M.A.S.; Abshar, M. Battery-Less Short-Term Smoothing of Photovoltaic Generation Using Sky Camera. *IEEE Trans. Ind. Inform.* **2018**, *14*, 403–414. [CrossRef]
27. Hoke, A.F.; Shirazi, M.; Chakraborty, S.; Muljadi, E.; Maksimovic, D. Rapid Active Power Control of Photovoltaic Systems for Grid Frequency Support. *IEEE J. Emerg. Sel. Top. Power Electron.* **2017**, *5*, 1154–1163. [CrossRef]
28. Batzelis, E.I.; Kampitsis, G.E.; Papathanassiou, S.A. Power Reserves Control for PV Systems with Real-Time MPP Estimation via Curve Fitting. *IEEE Trans. Sustain. Energy* **2017**, *8*, 1269–1280. [CrossRef]
29. Li, X.; Wen, H.; Zhu, Y.; Jiang, L.; Hu, Y.; Xiao, W. A Novel Sensorless Photovoltaic Power Reserve Control with Simple Real-Time MPP Estimation. *IEEE Trans. Power Electron.* **2019**, *34*, 7521–7531. [CrossRef]
30. Riquelme-Dominguez, J.M.; Martinez, S. A Photovoltaic Power Curtailment Method for Operation on Both Sides of the Power-Voltage Curve. *Energies* **2020**, *13*, 3906. [CrossRef]
31. Ye, D.; Riquelme-Dominguez, J.M.; Martinez, S. Estimation of the Output Characteristic of a Photovoltaic Generator under Power Curtailment and Considering Converter Losses. *Electronics* **2022**, *11*, 1544. [CrossRef]
32. Zhong, C.; Zhou, Y.; Yan, G. Power reserve control with real-time iterative estimation for PV system participation in frequency regulation. *Int. J. Electr. Power Energy Syst.* **2021**, *124*, 106367. [CrossRef]
33. Riquelme-Dominguez, J.M.; García-López, F.D.P.; Martinez, S. Power Ramp-Rate Control via power regulation for storageless grid-connected photovoltaic systems. *Int. J. Electr. Power Energy Syst.* **2022**, *138*, 107848. [CrossRef]
34. Hou, G.; Ke, Y.; Huang, C. A flexible constant power generation scheme for photovoltaic system by error-based active disturbance rejection control and perturb & observe. *Energy* **2021**, *237*, 121646. [CrossRef]
35. Chang, J.; Du, Y.; Lim, E.G.; Wen, H.; Li, X.; Jiang, L. Coordinated Frequency Regulation Using Solar Forecasting Based Virtual Inertia Control for Islanded Microgrids. *IEEE Trans. Sustain. Energy* **2021**, *12*, 2393–2403. [CrossRef]
36. Li, Z.; Cheng, Z.; Si, J.; Zhang, S.; Dong, L.; Li, S.; Gao, Y. Adaptive Power Point Tracking Control of PV System for Primary Frequency Regulation of AC Microgrid with High PV Integration. *IEEE Trans. Power Syst.* **2021**, *36*, 3129–3141. [CrossRef]